Sol−Gel Template Synthesis and Characterization of $BaTiO_3$ and $PbTiO_3$ Nanotubes

Bernadette A. Hernandez, Ki-Seog Chang, Ellen R. Fisher,* and Peter K. Dorhout

Department of Chemistry, Colorado State University, Fort Collins, Colorado 80523

Received July 20, 2001
Revised Manuscript Received November 25, 2001

Advances toward nanoscale electronics have created interest in the effects of particle size on the properties of ferroelectric ceramics. These materials are employed for their dielectric, piezoelectric, electrostrictive, pyroelectric, and electro-optic properties, with applications for ferroelectrics accounting for ≈60% of the global market for high technology functional ceramics.[1,2] The desirable properties of ferroelectric ceramics arise from their noncentrosymmetric unit cells that produce a polarization state.[3] Understanding how the crystal structure and state of polarization are influenced by particle size is vital to the performance of ferroelectric ceramics in many applications.

Much of the current research on the sources of size effects in ferroelectrics has focused on tetragonal barium titanate ($BaTiO_3$) through investigations of ultra-fine grain powders (<1 μm) with few reports on lead titanate ($PbTiO_3$).[2] As grain size is reduced, there is a decrease in the tetragonal lattice ratio constant (c/a) for room-temperature crystal structures.[2,4−7] The main issue with categorizing this effect lies in the synthetic methods. Different synthetic techniques and calcination temperatures influence the grain growth, resulting in widely varying "critical sizes" of $BaTiO_3$. Ultra-fine dense ceramic powders are also difficult to prepare because of their high surface areas and agglomeration.[13,16] The reduction in size also changes the ferroelectric to paraelectric transition temperature ($T_c \sim 120$ °C) of $BaTiO_3$. Several researchers have reported a lowering of T_c with the synthesis of smaller particles.[2,5,6,8,9]

Two different dielectric behaviors are observed as the grain size decreases. For grain sizes ranging from about 50 μm to 0.8 μm, the dielectric constant generally increases with decreasing grain size.[2,7,10,11] Buessem et al. reported that the increase in permittivity was a result of the absence of 90° twinning, which gives rise to internal stress below T_c.[12] For grains smaller than 0.8 μm there is a decrease in dielectric constant, which is not yet fully understood. Arlt et al. have argued that this decrease resulted from changes in crystal structure from tetragonal to cubic with grain size reduction, while Frey et al. suggested that the decrease was the result of dielectric mixing of interior grain volumes with ferroelectric ordering in the presence of disordered grain-boundary regions.[10,13]

The effects of depolarization in small particles have been explained in terms of a randomly oriented surface charge layer that begins to dominate the highly ordered ferroelectric interior as particle size decreases.[5] Eventually, the particle reaches a critical size where polarization becomes zero. Accounting for depolarization and using Landau−Devonshire theory, Wang and co-workers reported a critical size of 44 nm for $BaTiO_3$ particles.[14] Frey et al. reported a smaller critical size and showed experimental ferroelectric behavior in ceramics having grain sizes of 40 nm.[13]

Our work aims to understand how nanoscaling influences ferroelectric properties and to determine the critical size where a ferroelectric nanostructure no longer behaves like the bulk material. This communication focuses on the synthesis and characterization of the first perovskite nanotubes made by sol−gel template synthesis. Here, we have applied the previously reported techniques for the synthesis of metal oxides to the synthesis of the perovskites.[17] Our interest lies primarily in determining how the high aspect ratio shape and size along with the dimensionality of the nanotubes influences ferroelectric behavior relative to submicrometer particles.

$BaTiO_3$ and $PbTiO_3$ nanotubes were prepared with a 0.8 M sol made by dissolving the metal acetate ($Ba(OAc)_2$ or $Pb(OAc)_2 \cdot 3H_2O$, Aldrich) in hot HOAc (62 °C). The solution was then allowed to cool to 24 °C. A second solution of purified $Ti(OPr^i)_4$ (Aldrich) and EtOH was added to the metal acetate solution. Masked Whatman anodisc membranes (200-nm pores) served as templates and were dipped into the sol for 1 min and then allowed to air-dry for 30 min.[18] The samples were calcined in air at a rate of 50 °C/h to 650 °C for Pb and to 700 °C

* To whom correspondence should be addressed. E-mail: erfisher@lamar.colostate.edu.

(1) Mitsui, T.; Tatsuzakai, I.; Nakamura, E., Eds. *An Introduction to the Physics of Ferroelectrics*; Gordon and Breach Science Publishers: New York, 1976.
(2) Akdogan, E. K.; Leonard, M. R.; Safari, A. *Size Effects in Ferroelectric Ceramics*; Nawala, H. S., Eds.; Handbook of Low and High Dielectric Constant Materials, Vol.; Academic Press: San Diego, CA, 1999; p 61.
(3) Jona, F.; Shirane, G. *Ferroelectric Crystals*; MacMillan: New York, 1962.
(4) Uchino, K.; Sadanaga, E.; Hirose, T. *J. Am. Ceram. Soc.* **1989**, *72*, 1555.
(5) Asiaie, R.; Zhu, W.; Akbar, S. A.; Dutta, P. K. *Chem. Mater.* **1996**, *8*, 226−234.
(6) Shih, W. Y.; Shih, W.-H.; Akasay, I. A. *Phys. Rev. B: Condens. Matter* **1994**, *20*, 15575.
(7) Cheung, M. C.; Chan, H. L. W.; Choy, C. L. *J. Mater. Sci.* **2001**, *36*, 381.
(8) Frey, M. H.; Payne, D. A. *Phys. Rev. B* **1996**, *54*, 3158.
(9) Sakabe, Y.; Wada, N.; Hamaji, Y. *J. Korean Phys. Soc.* **1998**, *32*, S260.
(10) Arlt, G.; Hennings, D.; de With, G. *J. Appl. Phys.* **1985**, *58*, 1619.
(11) Zhang, J.; Lee, B. I.; Besson, J. J.; Mann, L. In *Electronic Ceramic Materials and Devices*; American Ceramic Society: Westerville, OH, 2000; p 541.
(12) Buessem, W. R.; Cross, L. E.; Goswami, A. K. *J. Am. Ceram. Soc.* **1966**, *49*, 33. Buessem, W. R.; Cross, L. E.; Goswami, A. K. *J. Am. Ceram. Soc.* **1966**, *49*, 36.
(13) Frey, M. H.; Han, Z. X. P.; Payne, D. A. *Ferroelectrics* **1998**, *206−207*, 337.
(14) Wang, Y. G.; Zhong, W. L.; Zhang, P. L. *Soild State Commun.* **1994**, *90*, 329.
(15) Martin, C. R. *Science* **1994**, *266*, 1961.
(16) Yukawa, K.; Wakino, K. *Integr. Ferroelectr.* **1998**, *20*, 107.
(17) Lakshmi, B. B.; Dorhout, P. K.; Martin, C. R. *Chem. Mater.* **1997**, *9*, 857. Lakshmi, B. B.; Patrissi, C. J.; Martin, C. R. *Chem. Mater.* **1997**, *9*, 2544.

10.1021/cm010998c CCC: $22.00
Published on Web 01/10/2002

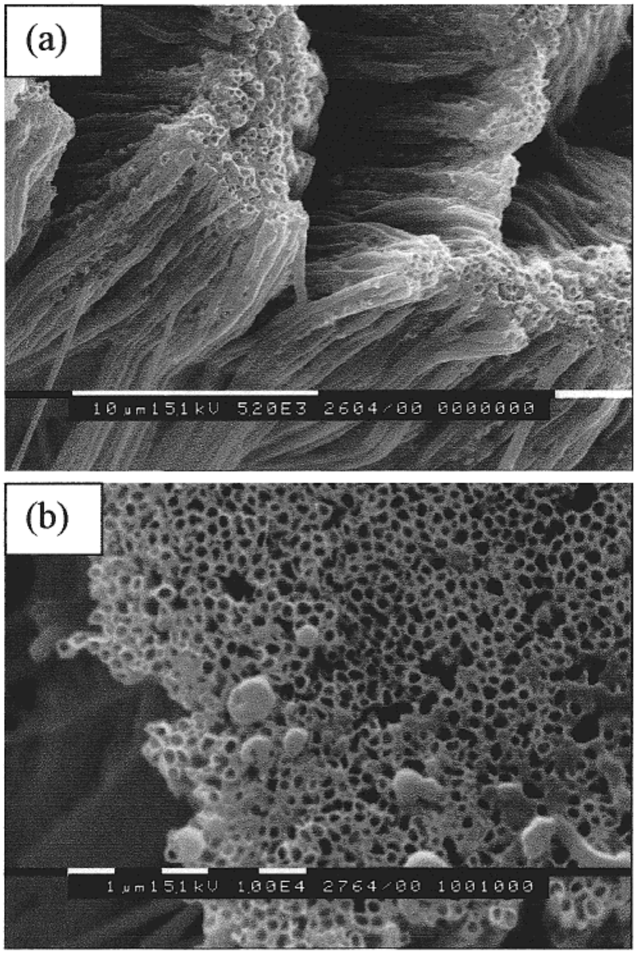

Figure 1. SEM images of perovskite nanotubes formed during sol−gel template synthesis using 200-nm alumina template membranes. (a) Side view showing bundle formation after the removal of the template. (b) Top view of $PbTiO_3$ bundle illustrating formation of open tubes with an outer diameter of 200 nm. With both materials, the nanotubes are ≈50 μm in length, which is the thickness of the template membrane.

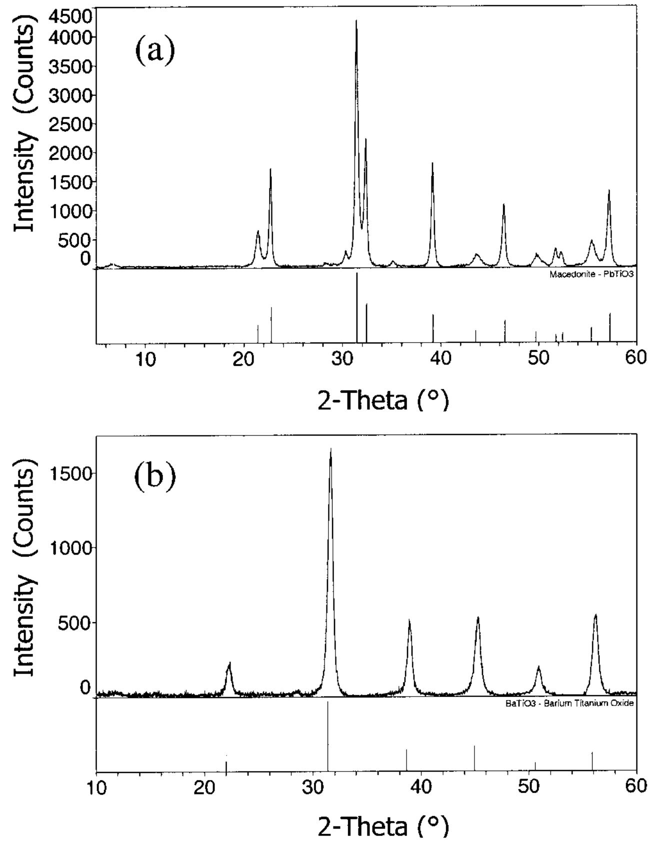

Figure 2. (a) Powder X-ray diffraction pattern for the bulk $PbTiO_3$ calcined to 650 °C was indexed to have the tetragonal structure. (b) Powder X-ray diffraction of the bulk $BaTiO_3$ calcined to 700 °C was indexed to have the cubic structure.

for Ba and then held at that temperature for 6 h, followed by cooling to 24 °C at 30 °C/h. After calcining, the template was removed with 6 M NaOH.[19] The remaining sol was used to make bulk powder samples of the perovskites for *d*-spacing comparison between electron diffraction patterns of the nanotubes and powder X-ray diffraction (XRD) from the bulk.

Scanning electron microscopy (SEM) images of the perovskite structures (Figure 1) reveal 50-μm-long tubes with 200-nm outer diameters. Figure 1a is a side view of $BaTiO_3$ and shows that the tubes bundle together after the removal of the template. Figure 1b is a top view of the $PbTiO_3$ structures, illustrating that the tubes are open-ended. By imaging different regions for both materials, we determined that the nanotubes are hollow throughout their entire length. Microanalysis by energy-dispersive spectroscopy (EDS) of the $BaTiO_3$ and $PbTiO_3$ tubes confirmed the presence of (Ba, Ti) and (Pb, Ti) for each perovskite. No Al peaks were found, thereby confirming that the amorphous AlO_x template had been fully removed.

Crystallographic characterization was performed with XRD, Raman, and electron diffraction obtained during transmission electron microscopy (TEM) analysis. Figure 2 shows the bulk powder XRD patterns for both perovskites. At the calcination temperature of 650 °C, $PbTiO_3$ crystallized in the tetragonal (ferroelectric) phase, while $BaTiO_3$ formed the cubic (paraelectric) phase at 700 °C. Raman spectra for both bulk compounds had peaks attributable to tetragonal structures.[5,20] The discrepancy between XRD and Raman data for $BaTiO_3$ suggests that the bulk material has more than one phase.[21] TEM and electron diffraction patterns for both perovskites (Figure 3) show that the tubes comprise small polycrystalline grains. The sizes of the grains are currently being investigated by XRD. To identify the phases of the perovskite tubes, the rings resulting from the electron diffraction were indexed to the XRD of the bulk material by the method of comparative *d*-spacing. Both electron and powder diffraction patterns had close index values, confirming that the phases of the bulk powder and nanotubes were similar.

(18) Templates were masked on one side with cellophane tape (3M) to prevent the formation of surface film, which inhibited the identification of tube or fiber formation.

(19) The template was attached to a paper towel with the masked side up using quick-dry epoxy. After setting, the sample was placed in the 6 M NaOH for 1 h to remove the template prior to SEM analysis.

(20) Li, S.; Condrat, R. A.; Spriggs, R. M. *Spectrosc. Lett.* **1988**, *21* (9−10), 969.

(21) Fately, W. G.; Dollish, F. R.; McDevitt, N. T.; Bently, F. F. *Infared and Raman Selection Rules For Molecular and Lattice Vibrations*; Wiley-Interscience: New York, 1972. On the basis of group theory, all four of the optical modes of cubic perovskite-type materials should be Raman-inactive, whereas seven of the optical modes for the polar tetragonal phase should be Raman-active.

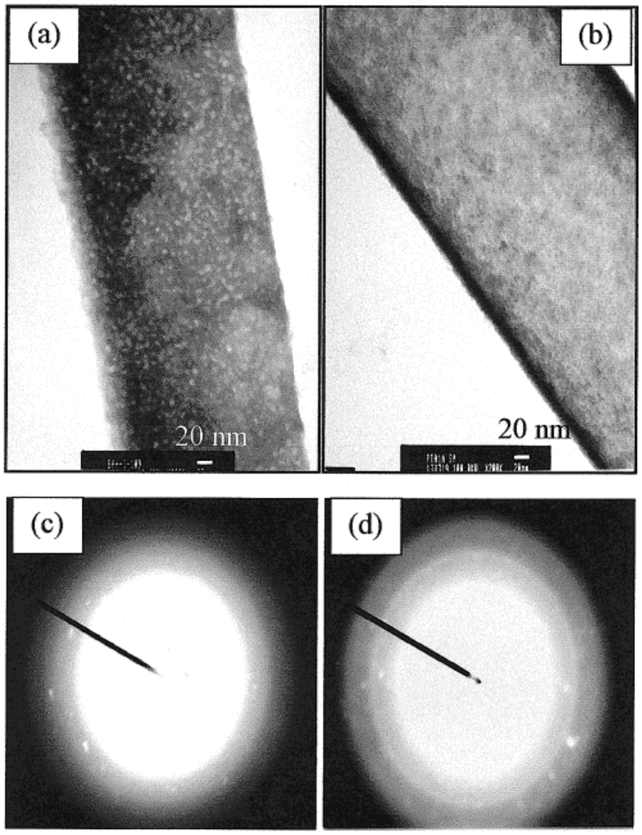

Figure 3. TEM images of $BaTiO_3$ (a) and $PbTiO_3$ (b) nanotubes. Both images show that the structures comprise small grains. Electron diffraction patterns for (c) $BaTiO_3$ nanotubes and (d) $PbTiO_3$ nanotubes. Ring patterns for both perovskites show the small grains are polycrystalline.

Preliminary dielectric data for the $BaTiO_3$ nanotubes supported by the alumina template were obtained to determine if there was a ferroelectric contribution from the tetragonal phase identified with Raman.[22] The dielectric temperature dependence of the alumina template at 30 °C has a permittivity (ϵ') of 1.64 which decreases to ≈1.1 as the temperature approaches 120 °C. The alumina template filled with $BaTiO_3$ has ϵ' of 22.3 at 30 °C which decreases to ≈2.0 as the temperature approaches 140 °C. No phase transition was observed in the range of 120−125 °C during the analysis, indicating that the nanostructures are paraelectric.[23] The curvature of the data was similar to previously reported data for thin films, ceramics, and submicrometer particles possessing the cubic phase.[1,3,11] We are currently acquiring dielectric data for the $PbTiO_3$ nanotubes.

In summary, this is the first report of sol−gel template synthesis of perovskite nanotubes. Bulk powder XRD identified the long-range crystal structure of $BaTiO_3$ as cubic, while Raman spectra showed that it contained a tetragonal component. Although it had some tetragonal phase, dielectric analysis showed it did not contribute to ferroelectric behavior in the nanotubes. Temperature dependence of the dielectric activity suggested that the paraelectric phase was obtained for $BaTiO_3$. The bulk powder of $PbTiO_3$ was found to have the tetragonal phase. Through comparative *d*-spacing, we assign the $BaTiO_3$ nanotubes to the cubic (paraelectric) phase and the $PbTiO_3$ to the tetragonal (ferroelectric) phase. We are currently exploring the tetragonal phase nanotubes for size effects. Through the sol−gel template synthesis, we can control the dimensions of the perovskite nanostructures, which will allow for a systematic study of size and ferroelectricity.

Acknowledgment. This work was supported by the Department of Energy, ER45791. The authors would like to thank the Electron Microscopy Center at Colorado State University for assistance in obtaining the SEM and TEM data.

CM010998C

(22) Permittivity (ϵ') measurements were taken on a TA Instruments DEA 2970 dielectric analyzer using parallel plate capacitor sensors. Samples underwent a temperature ramp/frequency sweep program mode. The temperature range measured was from 30 to 140 °C and the frequency range was 1−10000 Hz. During the analysis, 1 Hz was found to be the appropriate frequency to measure permittivity.

(23) The phase transition from ferroelectric to paraelectric behavior occurs around 120 °C for polycrystalline $BaTiO_3$. At this Curie temperature a maximum ϵ' can be measured.